

# Coherence of trapped one-dimensional (quasi-)condensates and continuous atom lasers in waveguides

N.P. Proukakis

*Department of Physics, University of Durham, South Road, Durham DH1 3LE, United Kingdom*

*\* E-mail: n.p.proukakis@durham.ac.uk*

We present a model for a continuous atom laser beam in a one-dimensional waveguide. The beam is formed by continuous raman outcoupling of a trapped one-dimensional (quasi-)condensate, which is created by imposing a tightly confining transverse optical potential on a three-dimensional magnetically trapped ultracold thermal gas. The trapped (quasi-)condensate is modelled by a stochastic Langevin equation, in which pumping arises naturally from the surrounding three-dimensional thermal cloud, which acts as its heat bath. When the outcoupling is turned on, such pumping leads to continuous replenishing of the (quasi-)condensate, and thus to a steady-state operation for the atom laser, which is described by a nonlinear Schrödinger equation, coupled to the Langevin equation for the (quasi-)condensate. This model is used to study the temporal and spatial evolution of the coherence length of the (quasi-)condensate and the atom laser over the entire system.

## I. INTRODUCTION

An atom laser is a device which emits an intense, directed coherent atomic beam in much the same way as a conventional (optical) laser emits a beam of coherent photons. Interest in such ‘devices’, whose potential applications include fields such as precision metrology, atom holography and nanotechnology, arose after the experimental realization of Bose-Einstein condensation (BEC) in trapped atomic alkali gases [1–3]. Although BEC need not necessarily be a prerequisite for the production of an atom laser, it was soon realized that a coherent atomic beam could be generated by the coherent extraction of a trapped BEC, thus leading to the first demonstration of a ‘rudimentary atom laser beam’ in 1997 [4,5]. In this pioneering experiment, atoms from a BEC trapped in a particular magnetic state were coherently extracted by means of pulsed radio-frequency (rf) transitions to a magnetically untrapped state; the outcoupled atoms then fell under gravity. Since then, a number of experimental groups have demonstrated the ability to produce pulsed [6,7], or quasi-continuous [8–12] atom lasers, with atoms usually extracted from the magnetically trapped state via rf or Raman transitions (although gravity-induced tunnelling from an optically trapped BEC has also been demonstrated as an outcoupling mechanism). The outcoupled atoms propagate away from the centre of the trap with an accelerated motion due to gravity, or at a constant speed due to the momentum imparted to the atoms by the two-photon Raman transitions. Raman outcoupling has the additional advantage of offering good spatial selectivity within the condensate. The removal of trapped atoms depletes the condensate and currently sets a very tight constraint on the duration of atom laser operation. Significant steps to overcome this limitation were recently carried out at MIT, where it was demonstrated that the time required for the creation of a reasonably-sized BEC can be significantly smaller than its lifetime [13]. This has enabled researchers to make a second BEC, merge it with an existing one, thus demonstrating the first real-time replenishing of a condensate. However, at the time of writing this paper, it is still unknown how such merging affects the coherence properties of the original condensate. All above discussion focuses on the production of an atom laser beam based on the coherent extraction of a ground-state BEC, and an interesting topic meriting further discussion is the possibility of creation of coherent atomic beams with different spatial modes, based on the coherent extraction of a non-ground-state BEC [14]. Finally, one should mention an alternative approach currently underway experimentally [15], which aims to create a continuous atom laser by evaporative cooling in a magnetic waveguide [16].

The coherence properties of trapped condensates have been studied experimentally using a variety of techniques. Spatial (equilibrium) properties have been studied by interfering two independent BEC’s [5], by studying two- [17] and three-body interactions [18], by spectroscopic techniques [19], and by interfering atoms extracted from different points within a single condensate [9], or at different times [20,21]. The temporal coherence of an atom laser beam extracted from a pre-formed BEC has been measured in [22], thus also yielding an upper limit for temporal phase

fluctuations within the condensate. On the theoretical side, the coherence properties of atom lasers have been studied in numerous publications, and an excellent review of the early literature on this topic (e.g. based on rate equations [23]) can be found in [24]. Our theoretical understanding of these issues has further improved following the successful analysis of a recent experiment by means of the Gross-Pitaevskii equation [21] and an in-depth discussion of output coupling based on Raman transitions [25]. However, such treatments are aimed at describing the coherence properties of an atom laser as it is extracted from a pre-formed (pure) condensate. These treatments hence suffer from two limitations: Firstly, they completely ignore the effect of thermal atoms which are inevitably present in the system and can lead to additional phase diffusion of the atom laser beam [26,27]. Perhaps more significantly for our current discussion, such treatments do not consider a re-pumping mechanism into the condensate, to compensate for the outcoupled atoms. These treatments are therefore not well suited for describing steady-state atom laser operation. The latter necessitates a mechanism pumping atoms into the condensate, and this is usually modelled phenomenologically [28–30]. In particular, in recent discussions [31,32], both trapped and outcoupled components are described by coupled nonlinear Schrödinger equations, with the trapped component additionally pumped from a thermal cloud, in such a manner, that the condensate is continually replenished during the outcoupling.

However, such pumping is assumed to be coherent, such that any atom falling into the magnetic trap becomes immediately part of the condensate, whereas we believe that a realistic pumping mechanism would, in general, introduce an additional phase diffusion of the condensate, as a result of the newly-pumped atoms. To account for this additional feature, one must combine the description of condensate formation based on quantum kinetic theory, with the process of coherent outcoupling. It is the aim of this paper to develop such a description and perform a qualitative and quantitative analysis of the coherence properties of a continuous one-dimensional atom laser. The results presented here are somewhat preliminary and will be further investigated in a subsequent publication. The important new feature of our model is that pumping arises naturally from the non-equilibrium treatment of the coupled dynamics of condensed and thermal atoms in a trap [33]. This gives rise to a Langevin equation for the growth of a condensate in contact with a heat bath [34] (note that such an approach differs considerably from previous stochastic treatments applied to similar issues [35,36]). The outcoupled atoms are then described by a nonlinear Schrödinger equation, which is coupled to the stochastic condensate field by (externally-induced) Raman coupling. The fluctuations inherent in the trapped component are then passed onto the atom laser beam, whose coherence properties we can thus determine.

This work focuses entirely on one dimensional systems, which are known to suffer from enhanced phase fluctuations and possess no off-diagonal long-range order. In particular, if such phase variations occur on length scales considerably smaller than the size of the system, then the system is known as a quasi-condensate [37,38]. This significant difference in the coherence properties of one-dimensional systems from the three-dimensional case usually encountered in current atom laser experiments indicates that our approach will yield estimates for the atom laser coherence which will be strongly dependent on the coherence properties of the original trapped (quasi-)condensate, and will thus, in general, not be directly applicable to current experiments. For this reason, our current work does not focus on the ‘absolute’ coherence of the atom laser, but rather on the dependence of the coherence properties of the output beam on the outcoupling procedure (given a particular coherence of the trapped system), and the change in the coherence properties of the trapped component due to the outcoupling. To some extent, such conclusions should also hold qualitatively for the three-dimensional systems. In this paper we discuss a continuous Raman output coupling scheme to a magnetically untrapped state, with the atoms leaving the ‘interaction region’ at the centre of the trap by means of the momentum imparted to them by the Raman lasers [10]. Throughout this work we assume that the entire system (condensate plus atom laser) remains kinematically one-dimensional, which is equivalent to an atom laser propagating in a transversely very tightly confining waveguide [39]. For technical reasons, the preliminary results presented in this paper are limited to the region of quasi-condensation, with parameters closely resembling those of a recent one-dimensional experiment [40]. The case of (almost) true condensation, and a more in-depth theoretical interpretation of the predictions of our model, will be discussed in a separate publication.

This paper is structured as follows. Sec. 2 discusses in detail the theoretical framework used to study the coherence properties of a (quasi-)condensate in a trap and the atom laser beam. In Sec. 3 we present results for the coherence length of the trapped component, prior to the outcoupling (Sec. 3.1) and after the outcoupling has been turned on (Sec. 3.2). Sec. 4 discusses the coherence length for the outcoupled component, and compares its behaviour at steady state to that of the trapped (quasi-)condensate. In particular, we discuss explicitly how the coherence length of the atom laser beam is modified by changing either the magnitude, or the phase of the external electromagnetic field (corresponding to the momentum imparted to the outcoupled atoms) producing the outcoupling. Finally, Sec. 5 presents some concluding remarks.

## II. THEORETICAL MODEL

In this section we present the theoretical framework to be used in the rest of the paper. Firstly, we describe the one-dimensional (quasi-)condensate in the trap.

### A. Trapped Component Only

Consider an ultracold magnetically trapped three-dimensional gas above the critical point, on which a laser beam is applied in such a manner that it provides an additional tightly-confining optical potential along two of the directions, in a manner similar to a recent experiment [41]. The laser beam can be arranged in such a manner that the potential ‘dimple’ it creates transversely to the waveguide has only one bound state below the chemical potential of the three-dimensional thermal cloud. In this case, the motion of the system becomes ‘frozen out’ along the transverse directions. The system thus becomes kinematically one-dimensional, but remains in contact with the three-dimensional thermal cloud, which acts as its heat bath. The dynamics of the order parameter  $\Phi(z, t)$  in the dimple is thus governed by [33,34]

$$i\hbar \frac{\partial \Phi(z, t)}{\partial t} = \left[ -\frac{\hbar^2 \nabla^2}{2m} + V^{\text{ext}}(z) - \mu - iR(z, t) + g|\Phi(z, t)|^2 \right] \Phi(z, t) + \eta(z, t), \quad (1)$$

where the external trapping potential in the weakly-confining direction is given by  $V^{\text{ext}}(z) = m\omega_z^2 z^2/2$ , and  $\mu$  is the effective chemical potential of the one-dimensional system. The one-dimensional coupling constant  $g$  is given by  $g = 4\pi\hbar^2\kappa/m$ , where  $\kappa$  corresponds to a one-dimensional scattering length; this is related to the usual three-dimensional scattering length  $a_{3D}$  by  $\kappa = a_{3D}/2\pi l_\perp^2$ , where  $l_\perp = \sqrt{\hbar/m\omega_\perp}$  is the harmonic oscillator length of the axially symmetric trap in the direction perpendicular to the waveguide axis  $z$ . Note that  $\Phi(z, t)$  corresponds to the **entire** field in the dimple, and not simply to the condensed component. The role of the thermal component is evident in the contributions  $iR(z, t)$  and  $\eta(z, t)$ . Physically, the function  $iR(z, t)$  describes the pumping of the one-dimensional gas from the surrounding reservoir, and  $\eta(z, t)$  corresponds to the associated noise with Gaussian correlations. In the classical field approximation [33,34] (which is well-satisfied in current experiments), these are given by

$$iR(z, t) = -\frac{\beta}{4}\hbar\Sigma^K(z) \left( -\frac{\hbar^2 \nabla^2}{2m} + V^{\text{ext}}(z) - \mu + g|\Phi(z, t)|^2 \right), \quad (2)$$

$$\langle \eta^*(z, t)\eta(z', t') \rangle = \frac{i\hbar^2}{2}\Sigma^K(z)\delta(z - z')\delta(t - t'), \quad (3)$$

where  $\langle \dots \rangle$  denotes averaging over the realizations of the noise  $\eta(z, t)$ , and  $\beta = 1/(k_B T)$  as usual. Both above quantities depend on the Keldysh self-energy  $\hbar\Sigma^K(z)$  which arises physically from collisions that scatter an atom out of, or into the ‘heat bath’, and is given by

$$\begin{aligned} \hbar\Sigma^K(z) = & -4i \frac{g^2}{(2\pi)^5 \hbar^6} \int dp_1 \int dp_2 \int dp_3 \delta(p_1 - p_2 - p_3) \delta(\epsilon_1 - \epsilon_2 - \epsilon_3 + V_{ext}) \\ & \times (N(\epsilon_1) + 1) N(\epsilon_2) N(\epsilon_3) \end{aligned} \quad (4)$$

where  $\epsilon_i = (p_i^2/2m) + V_{ext}(z_i)$  and  $N(\epsilon_i) = [\exp(\beta(\epsilon_i - \mu)) - 1]^{-1}$  is the Bose occupation factor. The numerical techniques employed are discussed in Ref. [34], where it was also shown that the above expressions guarantee that the trapped gas relaxes to the correct equilibrium, as ensured by the fluctuation-dissipation theorem. To simplify the numerics, the noncondensed part in the dimple is here allowed to relax to the ‘classical’ value  $N(\epsilon) = [\beta(\epsilon - \mu)]^{-1}$ .

Fig. 1 shows the evolution of the total density profile in the one-dimensional trap at different relaxation times (after turning on the optical dimple), for a sodium (quasi-)condensate at  $T = 200nK$  and with trapping frequencies taken from a recent experiment [40]. The effect of the thermal contributions is obvious, since the equilibrium density profile differs considerably from the corresponding (zero-temperature) Thomas-Fermi solution obtained in the absence of noise.

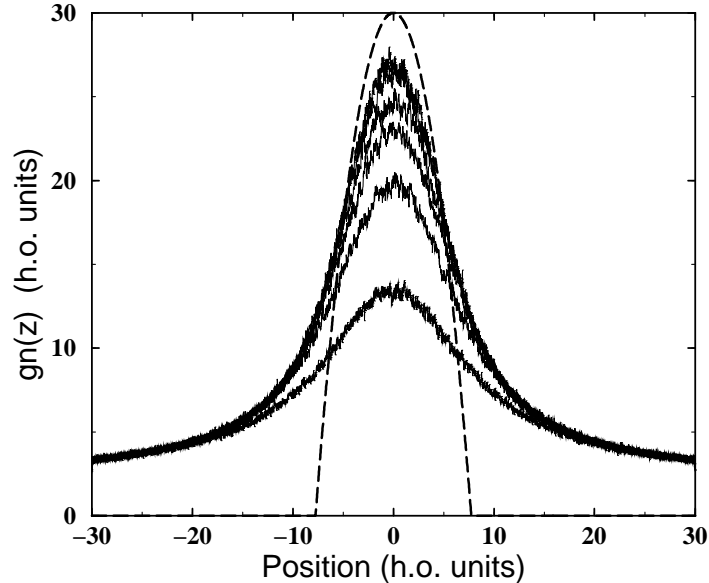


FIG. 1. Total density profile in the dimple after variable relaxation times, with  $t = 0$  corresponding to the time when the optical trap is switched on. From bottom to top (noisy curves):  $t_0/\tau = 4.8, 9.6, 14.4, 19.2, 28.8$  and  $38.4$  (corresponding to final relaxed value which is indistinguishable from that of  $28.8$ ). In this and subsequent figures, time and length are scaled to harmonic oscillator units, respectively  $\tau = \omega_z^{-1} = 45.5ms$  and  $l_z = \sqrt{\hbar/m\omega} = 11.2\mu m$ . The dashed line shows the corresponding Thomas-Fermi profile in the absence of thermal component (i.e. without noise), with the zero-temperature Thomas-Fermi radius acquiring a value  $R_{TF} = 7.74l_z$ . Throughout this paper, we use the magnetic trapping frequency  $\omega_z = 2\pi \times 3.5$  Hz, the transverse (optical) confining potential  $\omega_\perp = 2\pi \times 360$  Hz, and an effective one-dimensional chemical potential  $\mu = 30\hbar\omega_z$ . For  $^{23}Na$ ,  $m = 3.817 \times 10^{-26}kg$  and the three-dimensional scattering length is  $a_{3D} = 2.75nm$ . Throughout this paper, the surrounding thermal cloud is at a temperature  $T = 200nK$ . The discretization used is  $dx = 0.05l_z$  and  $dt = 0.0008\tau$ , which we have checked is sufficient to produce correctly converged results.

## B. Coupled Evolution of Trapped and Outcoupled Components

Having discussed how a one-dimensional (quasi-)condensate is produced, we next describe our model for a one-dimensional atom laser. After allowing the trapped component to relax to its equilibrium value, the outcoupling mechanism is turned on, leading to a continuous depletion of the (quasi-)condensate. Nonetheless, the presence of the additional pumping mechanism from the surrounding thermal cloud (which acts as its heat bath), leads to a steady-state population of the trapped component. An implicit crucial assumption made here is that the heat bath remains unaffected as it pumps atoms into the (quasi-)condensate, to compensate for the atoms lost from the trap due to outcoupling. This would indeed be the case (at least for short times) in the limit of very slow outcoupling and large initial thermal cloud. In our model, we envisage that the ultracold thermal cloud is continually replenished at a rate comparable to that of outcoupling. Then, our model is expected to be valid as long as the residual oscillations in the heat bath atom number (which indirectly affect the coherence of the trapped component and of the atom laser) are kept arbitrarily small, which we believe lies within current experimental capabilities. As noted earlier, we further assume that our entire system remains kinematically one-dimensional, which requires the optical dimple to extend over the entire range of our atom laser.

To model the raman outcoupling scheme, we follow the usual procedure of coupling the order parameter of the trapped system to a nonlinear Schrödinger equation for the outcoupled component. Such an approach has been already discussed in the literature [24,31,32], by making the further crucial assumption that the trapped component can be adequately described by a nonlinear Schrödinger equation with phenomenological pumping. Our treatment improves on such earlier attempts in that we explicitly include the effect of the thermal cloud on the trapped component by

means of a non-equilibrium theory based on the Schwinger-Keldysh formalism [33]. Hence, in our treatment pumping arises as a result of the relaxation of the system into its new confining potential.

The coupled evolution of the trapped  $\Phi_1(z, t)$  and outcoupled  $\Phi_2(z, t)$  components is thus determined by

$$i\hbar \frac{\partial \Phi_1(z, t)}{\partial t} = \left[ -\frac{\hbar^2 \nabla^2}{2m} + V_1^{\text{ext}}(z) - \mu + \delta - iR(z, t) + g_{11}|\Phi_1(z, t)|^2 + g_{12}|\Phi_2(z, t)|^2 \right] \Phi_1(z, t) + \Omega(z, t)\Phi_2(z, t) + \eta(z, t) \quad (5)$$

$$i\hbar \frac{\partial \Phi_2(z, t)}{\partial t} = \left[ -\frac{\hbar^2 \nabla^2}{2m} + V_2^{\text{ext}}(z) - \mu + g_{22}|\Phi_2(z, t)|^2 + g_{12}|\Phi_1(z, t)|^2 \right] \Phi_2(z, t) + \Omega^*(z, t)\Phi_1(z, t) . \quad (6)$$

Here  $g_{ii}$  correspond to the one-dimensional self-interactions of each component, whereas  $g_{12}$  is the mean-field interaction between the two components. For simplicity, we have taken  $g_{11} = g_{22} = g_{12} = g$  (defined earlier). The two components are coupled by the application of an external electromagnetic field via  $\Omega(z, t) = \Omega_0 e^{ikz}$ , where  $\Omega_0$  the strength of the Raman coupling and  $\hbar k$  the momentum imparted to the outcoupled atoms. Our description is limited to a one-dimensional atom laser in a **horizontal** waveguide, and thus ignores gravity. For  $^{23}\text{Na}$ , the trapped atoms are assumed to be in the  $|F, m_F\rangle = |1, -1\rangle$  state (for which  $V_1^{\text{ext}}(z) = m\omega_z^2 z^2/2$ ), whereas for simplicity we have chosen to outcouple the atoms to the untrapped  $|F, m_F\rangle = |1, 0\rangle$  state (for which  $V_2^{\text{ext}}(z) = 0$ ). All our simulations are performed at zero detuning ( $\delta = 0$ ) such that the outcoupling, which is peaked precisely at  $z = 0$ , occurs only in a very narrow region around the centre of the trap. An illustrative discussion of the effect of changing the detuning can be found in [42].

Fig. 2 shows the density profiles of the trapped and outcoupled components at steady state, for two different coupling parameters  $\Omega_0$ . We see clearly that the momentum kick imparted to the outcoupled atoms, leads to their propagation in the negative  $z$ -direction (note that absorbing boundaries have been used at the edges of our computational grid). Due to the mean field interaction between trapped and outcoupled components, such directional motion of the outcoupled atoms creates an asymmetry in the profile of the trapped atoms, which is more pronounced in the case of large  $\Omega_0$ . Since the outcoupling is primarily from the trap centre ( $\delta = 0$ ), this leads to a ‘‘double-peak’’ structure for the trapped atom density profile.

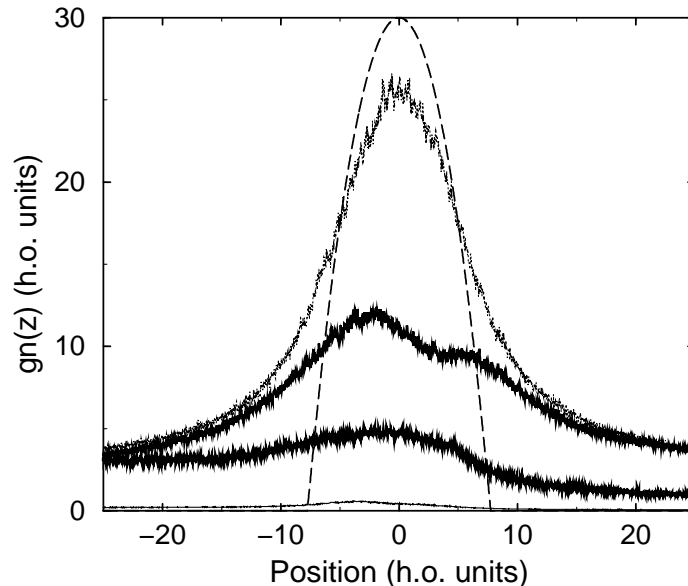


FIG. 2. Density profiles of trapped atoms (top two noisy curves) and outcoupled atoms (bottom two noisy curves) at steady state ( $t_0/\tau = 38.4$ ), in the limit of (i) ‘weak outcoupling’:  $\Omega_0 = 0.5\hbar\omega_z$  (thin noisy curves) and (ii) ‘strong outcoupling’:  $\Omega_0 = 5\hbar\omega_z$  (thick noisy curves), for  $\delta = 0$ . Also shown is the Thomas-Fermi profile (dashed line). Note that the equilibrium quasi-condensate profile prior to outcoupling essentially overlaps with the profile of the trapped atoms in the limit of ‘weak outcoupling’ shown here. In both cases the momentum imparted to the atoms is  $k = -5l_z^{-1}$ , corresponding to an atomic speed  $v = (\hbar k/m) \sim 1.2\text{mm/s}$  along the negative  $z$ -axis.

Having discussed our model and its predictions for the density profiles we now turn to the discussion of the coherence properties, which we investigate in terms of an appropriately defined coherence length.

### C. Definition of Coherence Length

The coherence properties of the system can be inferred from the behaviour of the normalized first-order off-diagonal correlation function defined by

$$g^{(1)}(z_0, t_0; z, t) = \frac{\langle \Phi_\alpha^*(z_0, t_0) \Phi_\alpha(z, t) \rangle}{\sqrt{\langle |\Phi_\alpha(z_0, t_0)|^2 \rangle \langle |\Phi_\alpha(z, t)|^2 \rangle}}, \quad (7)$$

where  $\langle \dots \rangle$  denotes averaging over noise realizations, and  $\alpha = 1, 2$  denote respectively the trapped and outcoupled components. Such a quantity can be calculated by numerical autocorrelation measurements. Fig. 3 shows the position dependence of the equal-time correlation function  $g^{(1)}(z_0, t_0; z, t_0)$  for the trapped component at the trap centre ( $z_0 = 0$ ), once it has relaxed to its equilibrium value in the absence of outcoupling. The observed rapid decay of the correlation function over the size of the system is clear evidence of quasi-condensation, as discussed in [43]. Since this closely resembles an exponential [44,45], we have chosen to define the coherence length,  $l_{coh}$  as the value of  $z$  for which this function decays to  $(1/e)$  (more generally  $g^{(1)}(z_0, t_0; (z_0 + l_{coh}), t_0) = (1/e)$ ). In this paper we will investigate the behaviour of  $l_{coh}$  (i) as a function of  $z_0$  for both trapped and outcoupled components, at fixed relaxation time  $t_0$ , and (ii) as a function of relaxation time  $t_0$ , for fixed position  $z_0$ . Note that by relaxation time we define the time elapsed from the moment that the tightly confining transverse potential is turned on.

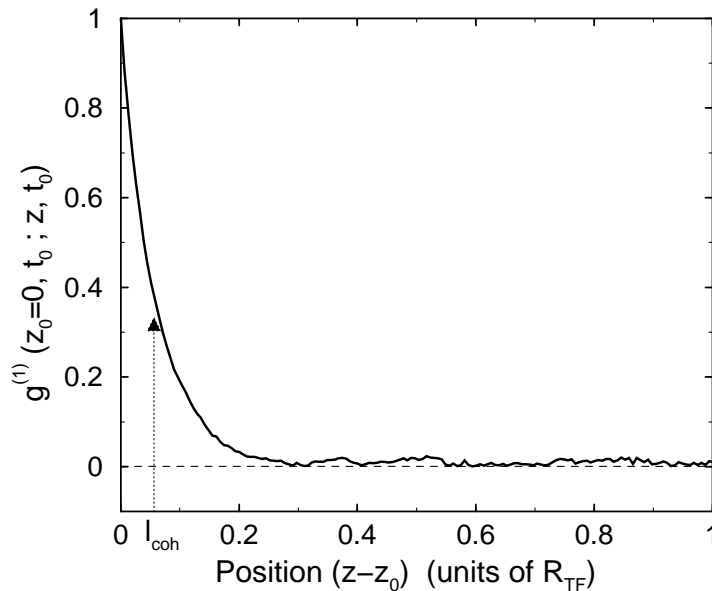


FIG. 3. Density profiles of trapped atoms (top two noisy curves) and outcoupled atoms (bottom two noisy curves) at steady state ( $t_0/\tau = 38.4$ ), in the limit of (i) ‘weak outcoupling’:  $\Omega_0 = 0.5\hbar\omega_z$  (thin noisy curves) and (ii) ‘strong outcoupling’:  $\Omega_0 = 5\hbar\omega_z$  (thick noisy curves), for  $\delta = 0$ . Also shown is the Thomas-Fermi profile (dashed line). Note that the equilibrium quasi-condensate profile prior to outcoupling essentially overlaps with the profile of the trapped atoms in the limit of ‘weak outcoupling’ shown here. In both cases the momentum imparted to the atoms is  $k = -5l_z^{-1}$ , corresponding to an atomic speed  $v = (\hbar k/m) \sim 1.2\text{mm/s}$  along the negative  $z$ -axis.

### III. COHERENCE LENGTH OF TRAPPED SYSTEM

#### A. Without Outcoupling

Initially we discuss the relaxation of the trapped component to its equilibrium value in the dimple prior to the outcoupling. Fig. 4(a) shows the temporal evolution of the coherence length at various positions in the trap. It is seen clearly that  $l_{coh}$  grows significantly at the trap centre and remains mostly unaffected at the edges of the trap (where there are only thermal atoms present). The dependence of  $l_{coh}$  on position in the trap at various times can also be seen in Fig. 4(b), which confirms the anticipated result that the coherence length is largest at the trap centre (where the quasi-condensate density is maximum).

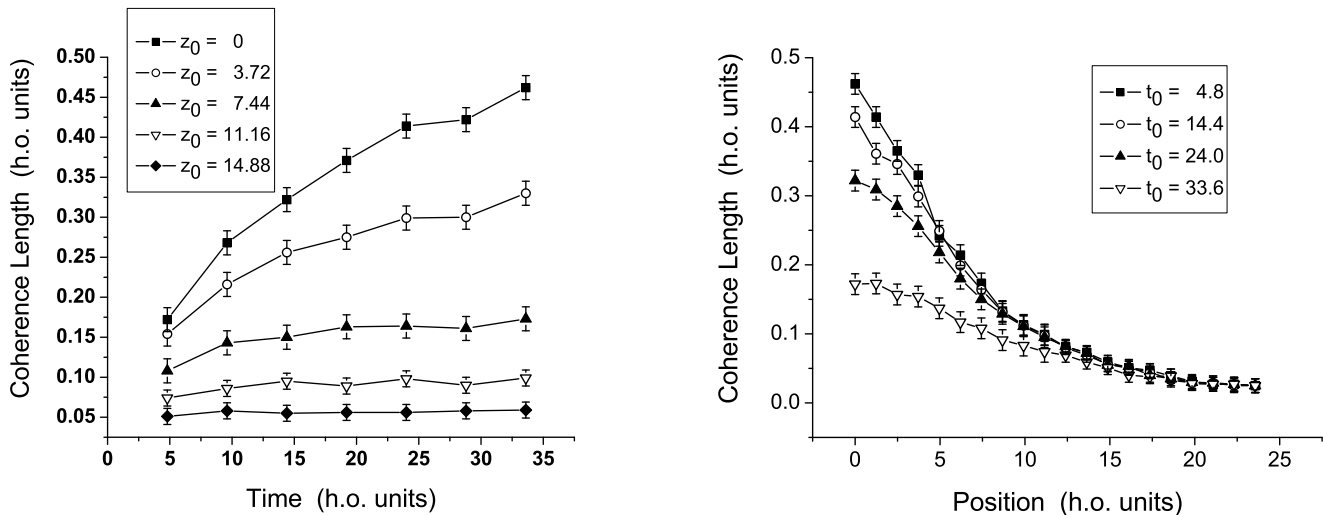


FIG. 4. Behaviour of the coherence length of the trapped component without output coupling (a) as a function of relaxation time  $t_0$ , at fixed points  $z_0$  in the trap; from top to bottom:  $z_0/l_z = 0$  (i.e. trap centre, squares), 3.72 (hollow circles), 7.44 (i.e. edge of Thomas-Fermi profile, upper triangles), 11.16 (hollow lower triangles) and 14.88 (rhombus). (b)  $l_{coh}$  as a function of position  $z_0$  for different relaxation times  $t_0/\tau = 4.8$  (squares), 14.4 (hollow circles), 24 (upper triangles) and 33.6 (hollow lower triangles). As a guide to the eye, neighbouring data points have been connected by straight lines.

#### B. With Outcoupling

The coherence length of the trapped component can decrease dramatically once the outcoupling is turned on, as a result of the removal of coherent atoms from the trap centre where the Raman transition resonance condition is satisfied. The values of the coherence length of the trapped component once steady state is reached between pumping and outcoupling are (potentially much) lower than the original values prior to outcoupling, because the atoms pumped from the surrounding thermal cloud to compensate for the atoms lost due to the outcoupling mechanism, do not necessarily share the same phase as the trapped atoms before their outcoupling. This is shown clearly in Fig. 5(a), which also demonstrates that the decrease in coherence is more dramatic at the trap centre (since atoms are mostly removed from that region) and essentially negligible outside the Thomas-Fermi radius of the system. Fig. 5(a) focuses on the regime of strong outcoupling where these effects are pronounced. In a typical experiment, one might seek to minimize the perturbations on the trapped component due to the outcoupling, and such a case (corresponding to the ‘weak outcoupling’ of Fig. 2(b)) will be further considered in Sec. 4.

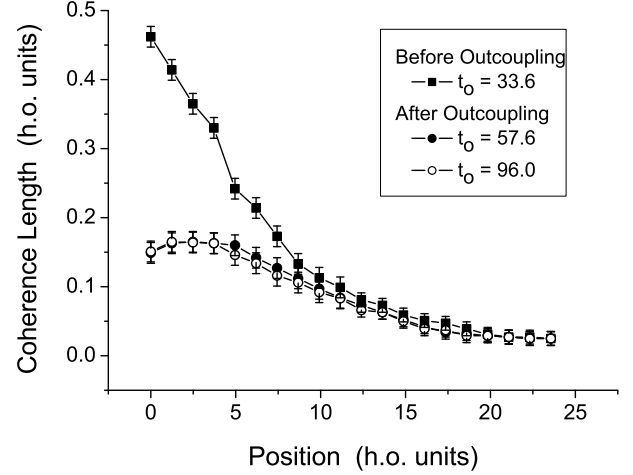
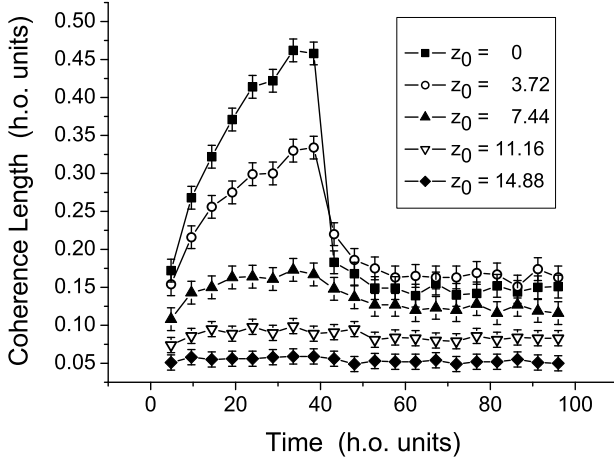


FIG. 5. Behaviour of the coherence length of the trapped component with ‘strong outcoupling’ ( $\Omega_0 = 5\hbar\omega_z$ ) in the limit of ‘large momentum kick’  $|k| = 5l_z^{-1}$ : (a)  $l_{coh}$  versus time at points  $z_0/l_z = 0$  (squares), 3.72 (hollow circles), 7.44 (upper triangles), 11.16 (hollow lower triangles) and 14.88 (rhombus). (b)  $l_{coh}$  versus position  $z_0$  at steady state (filled and hollow circles corresponding respectively to  $t_0/\tau = 57.6$  and 96.0). Outcoupling starts at  $t_0/\tau = 38.4$ . Shown also with squares is the coherence length attained before outcoupling ( $t_0/\tau = 33.6$ ).

Fig. 5(b) shows the dependence of the coherence length of the trapped component on position, once steady state has been reached. Apart from the rapid decrease of the coherence length due to the outcoupling procedure, we find that the coherence length is no longer maximum at the trap centre, but this maximum is now slightly offset along the  $z$ -axis. This reflects the fact that the maximum of the quasi-condensate density is slightly offset from its original value (as seen in Fig. 2; note that the positive  $z$ -axis of Figs. 3-9 corresponds to the negative  $z$ -axis of Fig. 2), due to the asymmetry created from the mean-field interaction between trapped and outcoupled atoms as a result of the directional motion of the outcoupled component.

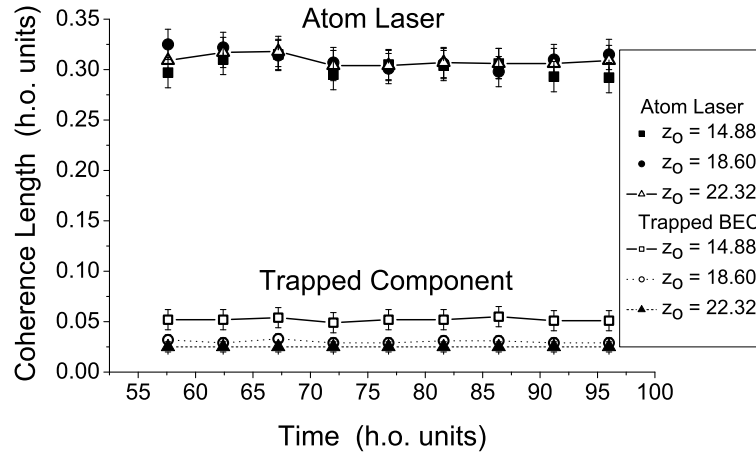


FIG. 6. Coherence length of an atom laser beam as a function of relaxation time  $t_0$  for three different points, located well outside the Thomas-Fermi region:  $z_0/l_z = 14.88$  (squares), 18.6 (circles) and 22.32 (hollow triangles), with the last data points connected by a solid line. The corresponding values of  $l_{coh}$  for the trapped component are also plotted for comparison (using similar symbols). As above,  $\Omega_0 = 5\hbar\omega_z$  and  $|k| = 5l_z^{-1}$ .



#### IV. COHERENCE LENGTH OF ATOM LASER BEAM

In order to discuss the coherence of an atom laser, we now perform the same type of analysis for the outcoupled component. Fig. 6 shows the coherence length of the atom laser beam as a function of time for particular points along the beam, chosen such that they lie well outside the Thomas-Fermi region where the interaction with the trapped quasi-condensate significantly affects its behaviour. From this figure, we deduce that the atom laser is essentially operating under steady-state conditions. Fig. 7 shows the position dependence of the coherence length of the trapped and outcoupled components at steady state, over the entire range of the trap. The coherence length of the outcoupled component is found to change considerably within the region where the trapped component exhibits significant coherence (ie essentially within the Thomas-Fermi radius of the quasi-condensate), and reaches a steady-state value far away from the center of the trap. On the contrary, the coherence length of the trapped component (apart from the minor increase at small values of  $|z|$  due to the asymmetry in the quasi-condensate density profile discussed above) decreases significantly as we move away from the centre of the trap. This shows that the outcoupled component acts as an atom laser, in the sense that it has a reasonably constant coherence length both in space and in time.

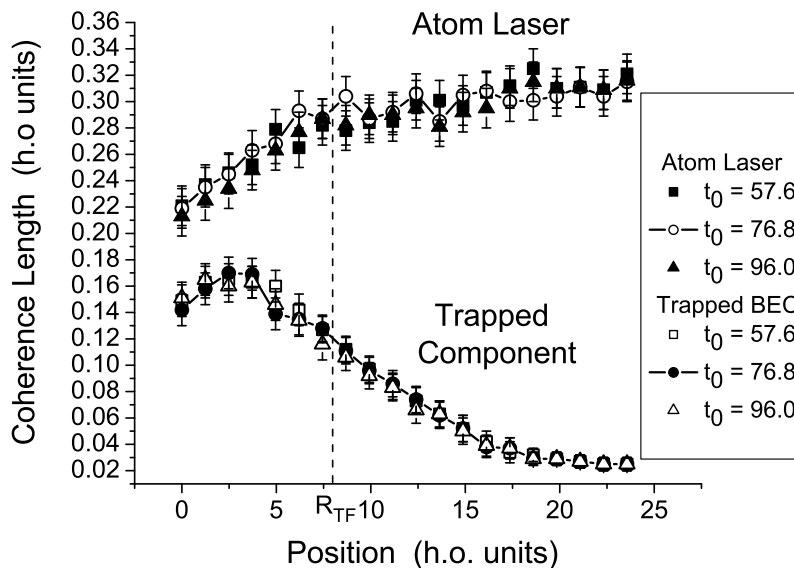


FIG. 7. Steady state dependence of the coherence length of trapped (lower branch) and outcoupled (upper branch) atoms on position ( $\Omega_0 = 5\hbar\omega_z$ ,  $|k| = 5l_z^{-1}$ ). Each curve is composed of three essentially overlapping sets of values corresponding to  $t_0/\tau = 57.6, 76.8$  and  $96.0$ , with the intermediate data points joined by straight lines. The dotted line indicates the position of the Thomas-Fermi radius.

All figures shown so far focused on the case of strong outcoupling which heavily depletes the quasi-condensate (since, in this limit, effects become more noticeable). On the contrary, the situation of most experimental interest is likely to be that in which the trapped component is only slightly perturbed by the outcoupling. This regime is discussed in Fig. 8 which plots the position dependence of the coherence length of both quasi-condensate and atom laser, for two different coupling strengths  $\Omega_0$ , focusing on the region of interest sufficiently far from the trap centre. The coherence length of the trapped component decreases rapidly towards the edges of the trap (since there is no off-diagonal long range order in one dimension) and is larger in the case of weaker outcoupling, since this leads to less depletion of the quasi-condensate (with the effect more pronounced within the Thomas-Fermi region which is not shown here). We believe that it is for the same reasons, that we find a longer steady state atom laser coherence length in the case of stronger outcoupling (see also [46]).

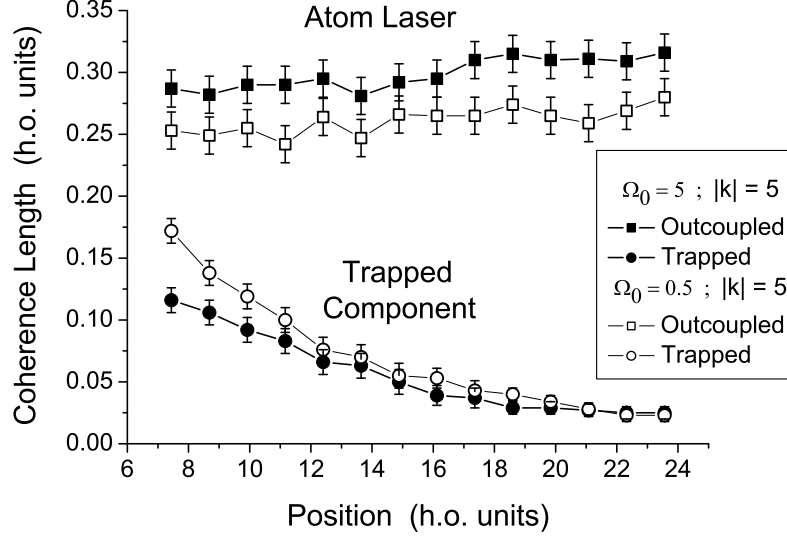


FIG. 8. Steady state ( $t_0/\tau = 96.0$ ) coherence length of quasi-condensate (lower branch, denoted by circles) and atom laser (upper branch, denoted by squares) as a function of position  $z_0$  for two different outcoupling strengths  $\Omega_0$ , for points outside the Thomas-Fermi radius ( $z_0 > R_{TF}$ ): (i) ‘Weak Outcoupling’  $\Omega_0 = 0.5\hbar\omega_z$  (hollow symbols) and (ii) ‘Strong Outcoupling’  $\Omega_0 = 5\hbar\omega_z$  (filled symbols). In both cases,  $|k| = 5l_z^{-1}$ .

Finally, Fig. 9 investigates the effect of imparting different ‘momentum kicks’  $k$  to the outcoupled atoms, at a constant outcoupling rate  $\Omega_0$ . The coherence length of the trapped component in the region  $z_0 < 12l_z$  is found to be somewhat larger in the limit of smaller momentum kicks. A possible interpretation, may be the following: since the outcoupled atoms leave the central ‘interaction region’ at a slower rate, the non-markovian nature of the mean field interactions between the two components [30] ensures that there is always a larger fraction of trapped atoms in this case, and hence more coherence within the trapped component. On the other hand, the coherence length of the atom laser beam is significantly increased for larger momenta, due to the increased speed of propagation of the outcoupled atoms in the waveguide.

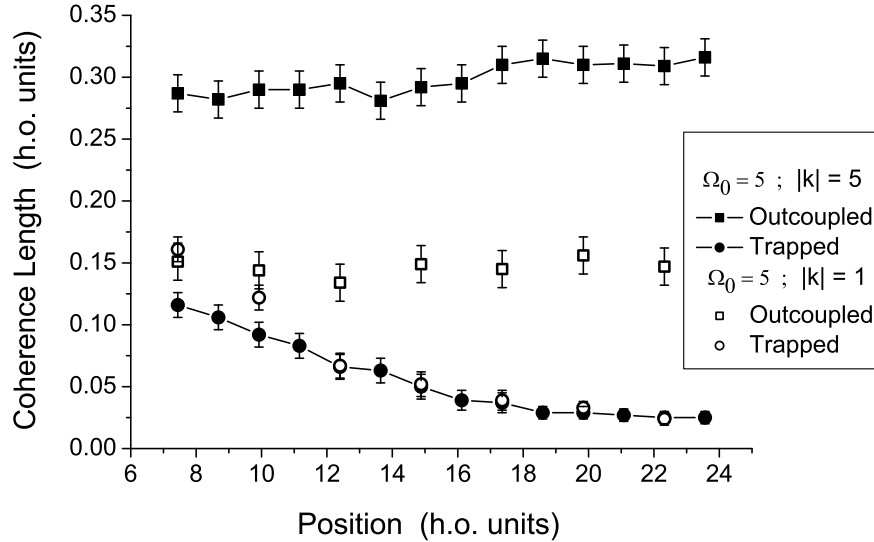


FIG. 9. Steady state ( $t_0/\tau = 96.0$ ) coherence length of quasi-condensate (denoted by circles) and atom laser (denoted by squares) outside the Thomas-Fermi radius as a function of position, for two different values of imparted momentum kicks to the outcoupled atoms, in the limit of ‘strong outcoupling’  $\Omega_0 = 5\hbar\omega_z$ : Filled symbols are the same as in Fig. 8 and indicate ‘large momentum kick’  $|k| = 5l_z^{-1}$  ( $v \sim 1.2mm/s$ ), whereas hollow symbols stand for ‘small momentum kick’  $k = l_z^{-1}$  ( $v \sim 0.24mm/s$ )

## V. CONCLUSIONS

The coherence properties of an atom laser beam are still only partially understood, despite significant work done on this field both experimentally and theoretically over the past few years. In this paper, we have focused on a one-dimensional atom laser beam in a tightly-confining waveguide, and we have shown that it can indeed maintain a reasonably constant coherence length in both space and time, in the region sufficiently far away from the centre of the trap (where the perturbations due to interactions with the trapped coherent component are minimized). Our system was assumed to be kinematically one-dimensional, and thus our analysis completely suppressed the effect of the transverse directions of the waveguide in which the atom laser propagates. In three-dimensional systems, the effects of the transverse modes can become significant, as discussed in [47,48]. Our values for the coherence length of the atom laser beam are considerably smaller than the corresponding three-dimensional systems, because it is well-known that phase fluctuations in low-dimensional systems can be strongly enhanced, leading to the appearance of quasi-condensation (that is, condensation with rapidly varying phase over the size of the system), as opposed to true condensation which arises in three-dimensional systems. In principle, this ‘defect’ can be cured, by working in that region of the phase diagram, where one essentially obtains ‘true BEC’ [49]. A further limitation of the approach discussed in this paper is that for computational reasons, the thermal cloud was treated classically, which means that its size was slightly overestimated, leading to a minor underestimate in the coherence properties of our system. Nonetheless, simulations of the full quantum theory have shown this effect to be a rather minor correction, at least for the parameters considered here [43].

Notwithstanding the above remarks, we consider our current contribution as yet another important step in the description of the coherence properties of atom lasers since, to the best of our knowledge, our work is the first qualitative and quantitative comparison of the coherence length of (quasi-)condensates and atom lasers beyond the usual mean field treatments. The analysis presented in this paper is based on somewhat preliminary results, and we intend to further investigate and support our conclusions in a subsequent publication. Furthermore, we are currently investigating the related issues of coherence time and linewidth of such atom lasers for experimentally relevant parameters (and in the limit of almost pure condensation), and such results will be presented elsewhere.

## ACKNOWLEDGEMENTS

I am indebted to Professor Henk Stoof for suggesting the application of the particular stochastic field method to study the coherence properties of atom lasers, and for his invaluable comments during the early stages of this work. I would also like to acknowledge computational assistance from Mark Leadbeater, and the hospitality of the Benasque Center for Science, where I had the opportunity to discuss my results with various participants of the ‘Physics of Ultracold Dilute Atomic Gases’ Workshop. Funding for this work was provided by the UK EPSRC.

- 
- [1] Anderson M. H., Ensher, J. R., Matthews, M. R. et al., 1995 *Science* **269**, 198.
  - [2] Davis, K. B., Mewes M. O., Andrews, M. R. et al., 1995, *Phys. Rev. Lett.* **75**, 3969.
  - [3] Bradley C. ,C., Sackett, C. A., Tollett, J. A. et al., 1995 *Phys. Rev. Lett.* **75**, 1687; Bradley C. ,C., Sackett, C. A. and Hulet R.G., 1997, *Phys. Rev. Lett.* **78**.
  - [4] Mewes, M. O. et al., 1997, *Phys. Rev. Lett.* **78**, 582.
  - [5] Andrews, M. R., Townsend, C. G., Miesner, H. J. et al., 1997, *Science* **275**, 637.
  - [6] Anderson, B. P. and Kasevich, M. A., 1998, *Science*, **282**.
  - [7] Martin, J. L. et al., McKenzie, C. R., Thomas, N. R. et al., 1999, *J. Phys. B* **32**, 3065.
  - [8] Bloch, I. et al., 1999, *Phys. Rev. Lett.*, **82**, 3008
  - [9] Bloch I., Hänsch, T.W. and Esslinger, T., 2000, *Nature* **403**, 166.
  - [10] Hagle, E. W., Deng, L., Kozuma, M. et al., 1999, *Science* **283**, 1706.
  - [11] Minardi, F., Fort, C., Maddaloni, P., 2000, *Proceedings of the 27<sup>th</sup> School of Quantum Electronics: Bose-Einstein Condensation and Atom Lasers*, Martelucci, S., Chester, A. N., Aspect, A. and Inguscio, M. (edt.) (Kluwer Academic).
  - [12] Le Coq, Y., Thywissen, J. H., Rangwala, S. A. et al., 2001, *Phys. Rev. Lett.* **87**, 170403.
  - [13] Hadzibabic, Z., Private Communication
  - [14] Yukalov, V. I., Yukalova, E. P. and Bagnato, V. S., 1997, *Phys. Rev. A* **56**, 4845.

- [15] Guery-Odelin, D., Private Communication.
- [16] Castin, Y., Dum, R., Mandonnet, E. et al., 2000, *J. Mod. Opt.* **47**, 2671.
- [17] Ketterle, W. and Miesner, H. J., 1997, *Phys. Rev. A*, **56**, 3291.
- [18] Hall, D. S., Matthews, M. R., Wieman, C. E. et al., 1998, *Phys. Rev. Lett.* **81**, 1543.
- [19] Stenger, J., Inouye, S., Chikkatur, A. P. et al., 1999, *Phys. Rev. Lett.* **82**, 4569.
- [20] Hagley, E. W., Deng, L., Kozuma, M. et al., 1999, *Phys. Rev. Lett.* **83**, 3112.
- [21] Trippenbach, M., Band, Y. B., Edwards, M. et al., 2000, *J. Phys. B*. **33** 47.
- [22] Köhl, M., Hänsch, T.W. and Esslinger, T. 2001, *Phys. Rev. Lett.* **87**, 160404.
- [23] Holland, M., Burnett, K., Gardiner, C. et al., 1996, *Phys. Rev. A* **54**, R1757.  
Wiseman, H. M., Martins, D. F., and Walls, D. F., 1996, *Quant. Semiclass. Opt.* **8**, 737.  
Guzman, A. M., Moore, A.M. and Meystre, P., 1996 *Phys. Rev. A* **53** 977.
- [24] Ballagh, R. J. and Savage, C. M., 2000 *Bose-Einstein Condensation: From Atomic Physics to Quantum Fluids, Proceedings of the 13th Physics Summer School*, Savage, C. M. and Das, M. (edt), (World Scientific, Singapore)
- [25] Edwards, M., Griggs, D. A., Holman, P. L. et al., 1999, *J. Phys. B* **32**, 2935.
- [26] Japha, Y., Choi, S., Burnett, K. et al., 1999, *Phys. Rev. Lett.* **82**, 1079.
- [27] Ruostekoski, J., Gasenzer, T. and Hutchinson, D. A. W., 2002, unpublished.
- [28] Hutchinson, D. A. W., 1999, *Phys. Rev. Lett.* **82**, 6.
- [29] Kneer, B., Wong, T., Vogel, K. et al., 1998, *Phys. Rev. A* **58**, 4841.
- [30] Hope, J. J., Moy, G. M., Collett, M. J. et al., 2000, *Phys Rev A* **61**, 023603.
- [31] Robins, N., Savage, C. and Ostrovskaya, E.A., 2001, *Phys. Rev. A* **64**, 043605.
- [32] Haine, S. A., Hope, J. J., Robins, N. P. et al., 2002, *Phys. Rev. Lett.* **88**, 170403.
- [33] Stoof, H. T. C., 1999, *J. Low Temp. Phys.*, **114**, 1.
- [34] Stoof, H. T. C. and Bijlsma, M. J., 2001, *J. Low Temp. Phys.*, **124**, 431.
- [35] Steel, M. J., Olsen, M. K., Plimak, L. I. et al., 1998 *Phys. Rev. A* **58**, 4824.
- [36] Graham, R., 2000, *Phys. Rev. A* **62**, 023609.
- [37] Popov, V. N., 1972, *Theor. Math. Phys.* **11**, 565; Popov, V. N., 1983, *Functional Integrals in Quantum Field Theory and Statistical Physics* (Reidel, Dodrecht), Chapter 6.
- [38] Petrov, D. S., Shlyapnikov, G. V. and Walraven, J. T. M., 2000, *Phys. Rev. Lett.* **85**, 3745.
- [39] Bongs, K., Burger, S., Dettmer, S. et al., 2001, *Phys. Rev. A* **63**, 031602(R).
- [40] Görlitz, A., Vogels, J. M., Leanhardt, A. E. et al., 2001, *Phys. Rev. Lett.* **87**, 130402.
- [41] Stamper-Kurn, D. M., Miesner, H. J., Chikkatur, A. P. et al., 1998, *Phys. Rev. Lett.* **81**, 2194.
- [42] Choi, S., Japha, Y. and Burnett, K., 2000, *Phys. Rev. A* **61**, 063606.
- [43] Al Khawaja, U., Andersen, J., Proukakis, N. P. et al. and Stoof, H. T. C., 2002, *Phys. Rev. A* **66**, 013615
- [44] Bogoliubov, N. M., Bullough, R. K., Kapitonov, V. S., 2001, *Europhys. Lett* **55**, 755.
- [45] Castin, Y, Dum, R, Mandonnet, E., et al., 2000, *J. Mod. Opt.* **47**, 2671.
- [46] Wiseman, H. M. and Vaccaro, J. A., 2002, *Phys. Rev. A* **65**, 043605 and *ibid.* 043606.
- [47] Gerbier, F., Bouyer, P. and Aspect, A., 2001, *Phys. Rev. Lett.* **86**, 4729.
- [48] Busch, T., Köhl, M., Esslinger, T. et al., 2002 *Phys. Rev. A* **65**, 043615.
- [49] Al Khawaja, U., Andersen, J., Proukakis, N. P. et al., 2002, unpublished.